Environmental Science & Technology

Article

pubs.acs.org/est

Enhancement of Fast CO_2 Capture by a Nano-SiO_2/CaO Composite at Ca-Looping Conditions

J. M. Valverde,*[,†] A. Perejon,[‡] and L. A. Perez-Maqueda[‡]

[†]Faculty of Physics, University of Seville, Avenida Reina Mercedes s/n, 41012 Seville, Spain

[‡]Instituto de Ciencia de Materiales de Sevilla (C.S.I.C.-Univ. Seville), Americo Vespucio 49, 41092 Seville, Spain

ABSTRACT: In this paper we show the performance of a new CO_2 sorbent consisting of a dry physical mixture of a Ca-based sorbent and a SiO_2 nanostructured powder. Thermo-gravimetric analysis (TGA) performed at conditions close to the Ca-looping process demonstrate that the rate of CO_2 capture by the mixture is enhanced during the fast carbonation stage of practical interest in applications. Moreover, the residual capture capacity of the mixture is increased. SEM/EDX, physisorption, and XRD analyses indicate that there is a relevant interaction between the nanostructured SiO_2 skeleton and CaO at high temperatures, which serves to improve the efficiency of the transfer of CO_2 to small reactive pores as well as the stability of the sorbent pore structure.

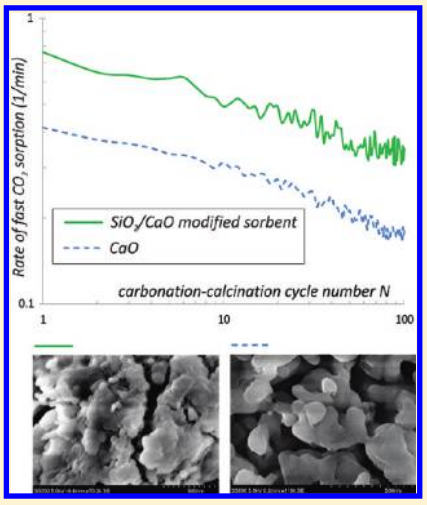

1. INTRODUCTION

The Ca-looping process involves the carbonation of CaO and the subsequent calcination of limestone ($CaCO_3$) to regenerate the sorbent.[1,2] Carbonation−calcination cycles are realized in practice by means of two interconnected fluidized beds operating under atmospheric pressure. The CaO powder reacts in a fluidized bed reactor (carbonator) with the CO_2 present in the gas to form $CaCO_3$ at temperatures around 600 °C. The spent sorbent is then regenerated by calcining it at temperatures around 900 °C in a second fluidized bed reactor (calciner). In the calciner, limestone decomposes to yield CaO and a concentrated stream of CO_2 ready to be stored. This process is currently implemented in large-scale pilot plants, showing considerable potential for reducing postcombustion CO_2 emissions.[3,4] It also has a promising application in the production of hydrogen from natural gas by means of the steam methane reforming process, which is enhanced by in situ capture of CO_2.[5]

Carbonation of CaO takes place in two stages.[3,6−8] A first fast carbonation stage consists of CO_2 sorption on the surface of CaO particles, which is controlled by chemical reaction (kinetic regime). Fast sorption finishes when the carbonate layer reaches a thickness of about 30−50 nm.[7] Then, it continues at a much slower rate controlled by diffusion of CO_2 through the carbonated layer. The stage of practical interest is fast carbonation since the sorbent must react with CO_2 over short contact times.[1] Ideally, the sorbents should react fast toward an optimum capture capacity and maintain it as the number of carbonation−calcination cycles is increased.[1,9] Yet the capture capacity of CaO decreases with increasing the number of cycles, which is attributed to the decrease of the reactive surface area as a result of sintering.[3,7,8] In a very recent work, Chen et al.[10] have presented a synthetic sorbent prepared by mixing rice husk ash (of high SiO_2 content) with calcined limestone in an aqueous solution. CO_2/SO_2 capture capacity was enhanced for an optimum SiO_2/CaO molar ratio of 0.2 under pressurized carbonation. In a previous work, Li et al.[11] had shown that a hydrated mixture of rice husk ash/CaO also exhibited enhanced carbonation conversion at atmospheric pressure for certain preparation conditions (hydration temperature of 75 °C, hydration time of 8 h, and SiO_2/CaO molar ratio of 1.0). The authors of these works argued that, because of the higher melting point of calcium silicates formed by the reaction between SiO_2 and $Ca(OH)_2$, the resistance to sintering was increased.[10] It is also remarkable that in their experiments, the carbonation time was 15 min in ref 11 and 25 min in ref 10. When the carbonation time was decreased to 10 min the sorbent performance was reduced.[10] As demonstrated by Wang et al.,[12] it could be also possible that CO_2 is sorbed by calcium silicates over long carbonation periods.

In our study, a fine $Ca(OH)_2$ powder (Merck) is used as original CO_2 sorbent. When this cohesive powder is fluidized, its macroscopic behavior is heterogeneous (Geldart C

Received: January 25, 2012
Revised: May 4, 2012
Accepted: May 8, 2012
Published: May 2, 2012

 © 2012 American Chemical Society dx.doi.org/10.1021/es3002426 | Environ. Sci. Technol. 2012, 46, 6401−6408

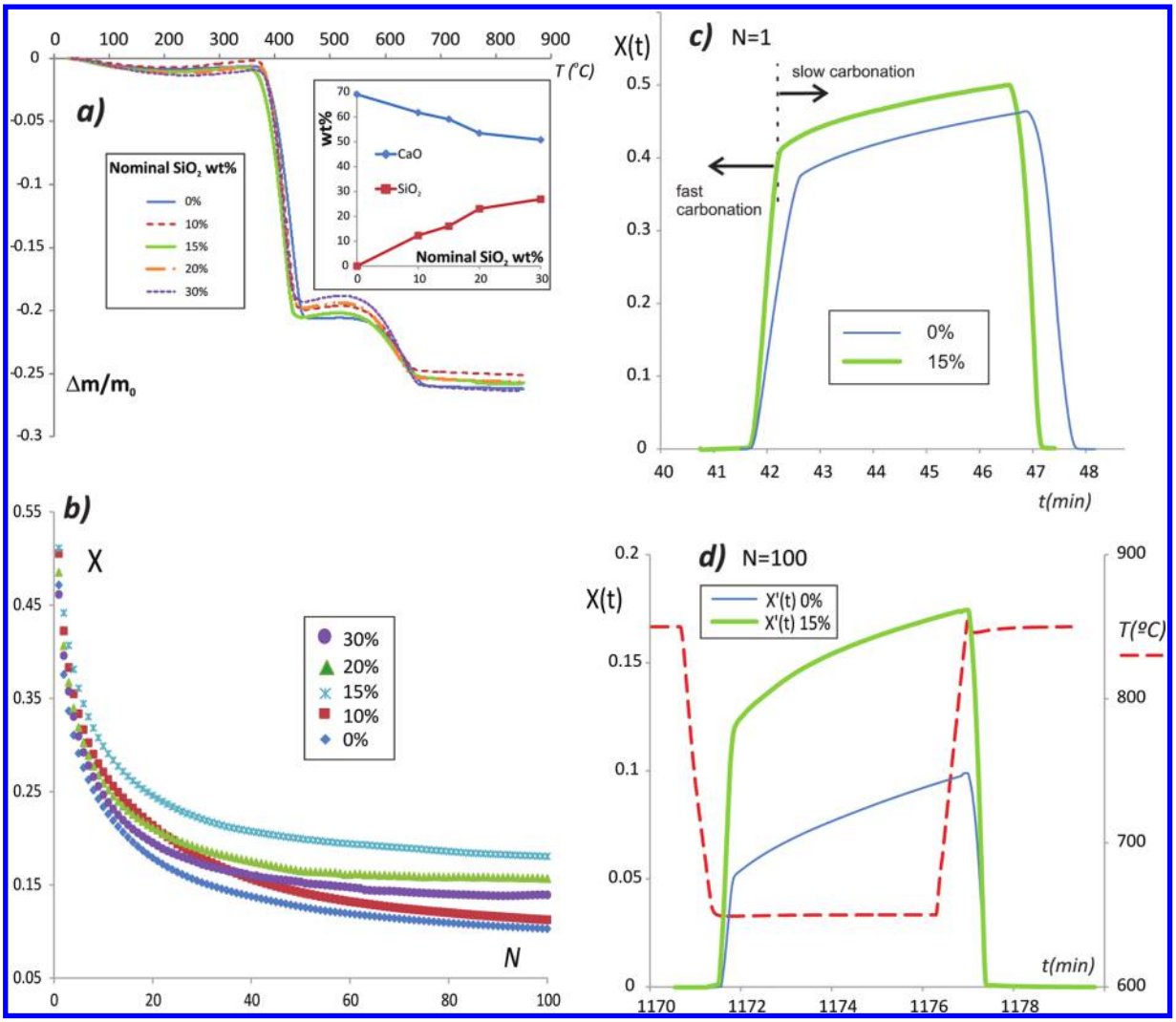

Figure 1. (a) Thermogram obtained during pretreatment of $Ca(OH)_2$ and nano-SiO_2/$Ca(OH)_2$ mixtures by heating them to 850 °C in a N_2 dry atmosphere (nominal wt% of SiO_2 in the freshly prepared mixtures is indicated). The inset shows the wt % (on the total weight of the freshly prepared samples) of SiO_2 and CaO remaining after pretreatment, which was calculated from this thermogram. (b) CO_2 capture capacity of the nano-SiO_2/CaO mixtures as the number N of carbonation−calcination cycles is increased (nominal SiO_2 wt % is indicated). Results from independent tests on different samples (not shown) demonstrated data reproducibility within a 10% relative variation. (c) and (d) Relative mass of CO_2 sorbed and desorbed as a function of time during carbonation−calcination cycles number 1 (c) and 100 (d) for CaO and a nano-SiO_2/CaO mixture (15 wt % SiO_2). Variation of temperature as a function of time is shown in (d) (right axis).

behavior[13]). Stable gas channels are developed through which the gas bypasses the bed, hindering the efficiency of the gas−solids contact. As reported in ref 14, the fluidizability of this powder is enhanced by dry mixing it with a nanostructured SiO_2 powder (Aerosil R974 supplied by Evonik Industries), which helps the destabilization of gas channels. Aerosil R974 is an amorphous silica manufactured by flame hydrolysis with a reported primary particle size of 12 nm and BET surface area of 200 m^2/g. Due to long pathways of primary nanoparticles in the flame reactor at high temperatures, these nanoparticles have extremely short life as individual particles. They form fractal aggregates, of size on the order of micrometers, wherein nanoparticles are permanently held together by strong chemical bonds due to sintering.[15] Subsequently, these aggregates join together due to attractive van der Waals forces, forming light and fluidizable agglomerates of size between tens and hundreds of micrometers and density of the order of tens of kg/m^3.[16,17] When $Ca(OH)_2$ is physically dry-mixed with the SiO_2 powder, SiO_2 nanostructured agglomerates become coated with the $Ca(OH)_2$ particles due to electrostatic charge transfer.[14,18] A test performed at ambient pressure and temperature (reported in 14) showed that the time for CO_2 breakthrough in the effluent gas from a fluidized bed was increased for the nano-SiO_2/$Ca(OH)_2$ mixture because of fluidization homogenization. Besides of the preparation method, a main difference with SiO_2/CaO sorbents presented elsewhere[10,11] is that the SiO_2 powder used in our work is nanostructured. As a result, it will be shown in the present manuscript that the rate of fast carbonation (taking just tens of seconds) and residual capture capacity are enhanced at Ca-looping conditions and atmospheric pressure for small values of the SiO_2/CaO molar ratio.

2. EXPERIMENTAL RESULTS

A Q5000IR TG analyzer (TA Instruments) with a fast infrared furnace and a high sensitivity balance (<0.1 μg) characterized by a minimum baseline dynamic drift (<10 μg) was used. The samples tested were the $Ca(OH)_2$ powder and dry physical mixtures of $Ca(OH)_2$ with nano-SiO_2 (nominal SiO_2

dx.doi.org/10.1021/es3002426 | Environ. Sci. Technol. 2012, 46, 6401−6408

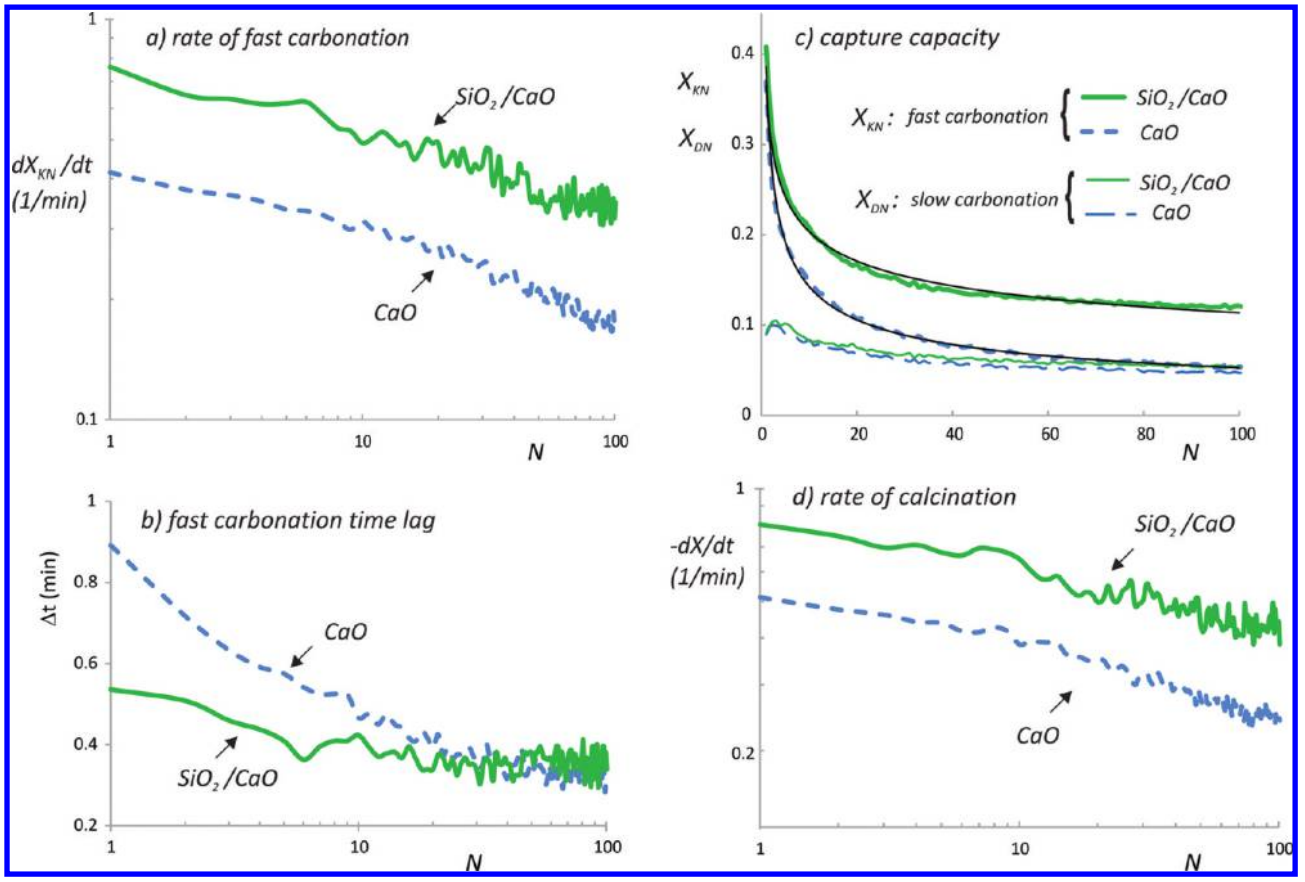

Figure 2. (a) Sorption rates in the fast carbonation stage as the number of carbonation−calcination cycles is increased. (b) Time of duration of the fast carbonation stage. (c) Capture capacities in the fast and slow carbonation stages, X_{KN} and X_{DN}, respectively. (d) Decarbonation rates during calcination. Results are shown for CaO and for a nano-SiO_2/CaO mixture (15 wt % SiO_2). Solid thin lines in (c) are best power law fits to the data: $X_{KN} = 0.365N^{-0.253}$ for the nano-SiO_2/CaO mixture and $X_{KN} = 0.386N^{-0.432}$ for CaO.

concentrations between 10% and 30% by SiO_2 weight on $Ca(OH)_2$ weight). The mass of the samples ranged between 10 and 20 mg.

Once the sample was placed in the TG balance, it was heated to 850 °C in a N_2 atmosphere (20 °C/min). As the temperature was raised, the sample went across dehydration and desorption of CO_2 as seen in the thermogram shown in Figure 1a. After preheating, the sorbent consisted thus of a mixture of CaO and nano-SiO_2 at weight percentages shown in the inset of Figure 1a. Once preheating was finished, the temperature was decreased to 650 °C and the sample was subjected to a flow (100 cm^3 min^{-1}) of a gas mixture of CO_2 (15% volume concentration) and air for 5 min. Then, the temperature was raised to 850 °C (heating rate 300 °C/min) and the sample was calcined in an air flow (100 cm^3 min^{-1}) during 5 min for decarbonation. After calcination, the temperature was decreased (cooling rate 300 °C/min) to proceed again with carbonation.

Data of the mass of CO_2 sorbed relative to the mass of CaO (capture capacity X) are plotted in Figure 1b as a function of the number of carbonation−calcination cycles N. $X(N)$ decreases with increasing N and tends to a residual value X_r around 0.1 for CaO, which is similar to the value typically reported for natural limestones.[19] The values of $X(N)$ for the nano-SiO_2/CaO mixtures become relatively higher as N is increased. The highest residual capacity is obtained for a 15 wt % of nano-SiO_2 (SiO_2/CaO molar ratio of 0.25), $X_r \simeq 0.18$, which is almost twice the residual capacity obtained for CaO. As discussed in ref 14 this SiO_2 percentage gives the optimum amount needed to achieve a maximum contact of the surface nano-SiO_2 with $Ca(OH)_2$ in the initial mixture.

Figure 1c and 1d show the relative mass of CO_2 sorbed and desorbed as a function of time during the first and last cycles (15 wt % SiO_2). As well documented in the literature,[3,6−8] carbonation takes place in two stages: an initial fast carbonation stage controlled by surface reaction and a subsequent slower stage controlled by diffusion. The presence of nano-SiO_2 has a relevant influence on the rate of sorption during fast carbonation (dX_{KN}/dt) and the rate of decarbonation during calcination ($-dX/dt$), which take place at a faster rate. This is clearly seen in Figure 2a and 2d, where dX_{KN}/dt and $-dX/dt$ are plotted versus N. Figure 2b illustrates the time lag of the fast carbonation stage (Δt). In the first cycle, fast carbonation for CaO takes about $\Delta t_{CaO} \simeq 50$ s, which is similar to the value reported for calcined samples of fine natural limestones in similar conditions.[7] Δt_{CaO} decreases with N and tends to $\Delta t_{CaO} \simeq 20$ s for large N (Figure 2b). On the other hand, Δt is initially smaller for the nano-SiO_2/CaO mixture ($\Delta t_{CaO} \simeq 30$ s) but it decreases at a slower rate as N is increased and tends to $\Delta t_{SiO2/CaO} \simeq 20$ s for $N > 20$, which is similar to Δt_{CaO} that keeps slowly decreasing even at large N. The data plotted in Figure 2c show the capture capacities during the fast stage (X_{KN}) and the slow stage (X_{DN}). There is a clear effect of nano-SiO_2 on the rate of decrease of X_{KN} with N as compared to the rate of decrease of X_{DN}, which is similar for both sorbents. X_{KN} decreases at a relatively higher rate in the case of the original

dx.doi.org/10.1021/es3002426 | Environ. Sci. Technol. 2012, 46, 6401−6408

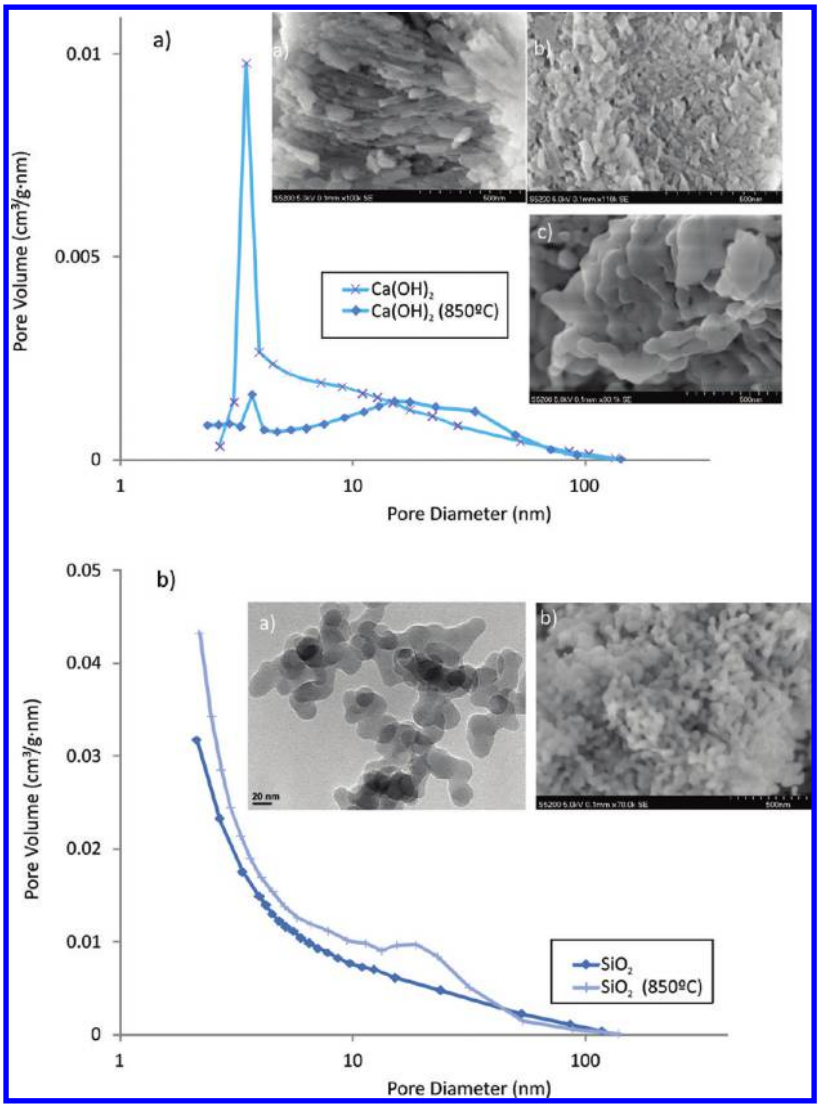

Figure 3. BJH desorption (dV/dD) pore volume distributions for the $Ca(OH)_2$ (a) and nano-SiO_2 powders (b) used in our study as received and after being heated to 850 °C. The inset of (a) shows SEM pictures of the surface of $Ca(OH)_2$ particles before (a and b) and (c) after thermal pretreatment (CaO). The inset of (b) shows a TEM picture of nano-SiO_2 agglomerates before thermal pretreatment (a) and a SEM picture after thermal pretreatment (b).

sorbent ($r_K \equiv -\Delta \ln X_{KN}/\Delta \ln N \simeq 0.432$), approaching X_{DN} for large N. In contrast, r_K is notably lessened for the nano-SiO_2/CaO mixture, being $r_K \simeq 0.253$, which is similar to the decay rate of the capture capacity in the diffusion regime. Thus, X_{KN} is kept at a relatively high value as compared with X_{DN} at large N for the modified sorbent. These results illustrate that fast capture capacity and sintering resistance are enhanced at conditions close to the Ca-looping process.

A relevant aspect of TGA experiments is the heating and cooling rates between cycles. The use of an infrared furnace in our TGA runs allowed us for heating and cooling the sample very quickly (300 °C min^{-1}), thus the carbonation−calcination transitions took place in just 40 s. To assess whether sintering in this period might influence the performance of the sorbent, the results reported by Borgwardt[20] can be used. The reduction of the specific surface area ΔS is expressed as a function of time t as $(\Delta S/S_0)^\gamma = Kt$ where S_0 is the initial specific surface area and K is the sintering rate constant, which increases with temperature T according to the law $\Delta \log K \propto -1/T$.[20] The exponent γ measured for CaO is $\gamma \simeq 2.7$.[20] In the case of CaO produced by thermal decomposition of $Ca(OH)_2$, it is $K \simeq 10^{-4}$ min^{-1} at 650 °C, $K \simeq 10^{-2}$ min^{-1} at 850 °C. Accordingly, no appreciable surface area reduction is expected in our experiments during the transitional periods (t = 40 s). On the other hand, heating rates typically employed in conventional TGA instruments (of about 50 °C min^{-1} or even smaller[21]) are likely to yield nonnegligible sintering in the transitional periods, which would affect the CO_2 capture performance.

The effect of heating the sorbents during pretreatment and subsequent calcination cycles on their BET surface area and pore size distribution (BJH method) was investigated by means of a TriStar II 3020 V1.03 physisorption analyzer operated by N_2 sorption at 77 K. This analysis was complemented by SEM observations using a HITACHI Ultra High-Resolution S-5200 equipped with an EDX spectroscopy unit (Bruker AXS Microanalysis GmbH) for chemical characterization of the sample. Figure 3 shows pore size distributions obtained for both the $Ca(OH)_2$ and nano-SiO_2 powders as received and after being preheated individually. The pore size distribution of the untreated $Ca(OH)_2$ powder (Figure 3a) has a pronounced

dx.doi.org/10.1021/es3002426 | Environ. Sci. Technol. 2012, 46, 6401−6408

peak at a pore size close to 3−4 nm in accordance with SEM images showing tiny crystals with a typical size of less than tens of nm (see inset of Figure 3a). The morphology of the $Ca(OH)_2$ surface is severely changed after heating due to sintering as seen in the inset of Figure 3a. Accordingly, the region in the pore size distribution comprising pore sizes smaller than 10 nm is flattened and the distribution weight is shifted toward larger pore sizes (Figure 3a). As regards nano-SiO_2, SEM images (inset of Figure 3b) show coalescence and growth of the nanoparticles in the agglomerates but changes in the pore size distribution are not relevant (Figure 3b). Pore size distributions of the mixtures are plotted in Figure 4. As

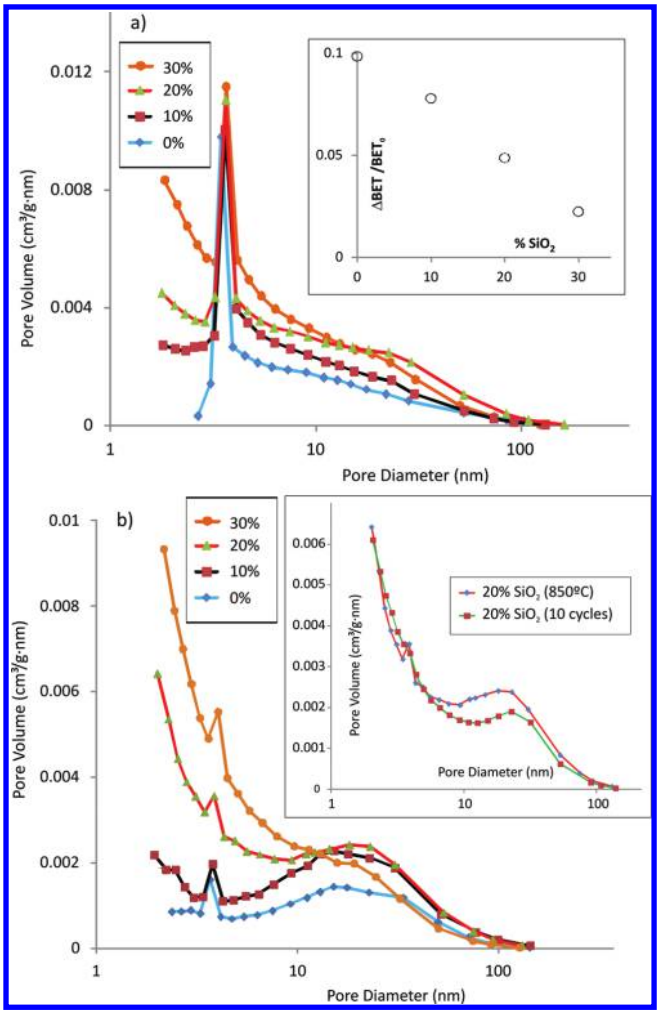

Figure 4. BJH desorption (dV/dD) pore volume distributions for $Ca(OH)_2$ and for the mixtures before (a) and after (b) being heated to 850 °C (wt % of nano-SiO_2 is indicated). The inset of (a) shows the relative decrease of BET surface area after heating the mixtures as a function of the SiO_2 wt %. The inset of (b) shows the pore volume distributions of a 20 wt % SiO_2 sample preheated at 850 °C and after 10 calcinations.

expected from the pore size distributions obtained for both powders individually, the mixtures containing a high percentage of nano-SiO_2 preserve a relatively larger amount of pores smaller than 10 nm after being heated. Accordingly, the relative decrease of the BET surface area caused by sintering (inset of Figure 4a) is lessened as the percentage of nano-SiO_2 is increased.

Physisorption measurements were also carried out after the powders were subjected in a furnace to 10 cycles changing the temperature between 650 and 850 °C as in TGA tests. The pore size distribution of the nano-SiO_2 powder remained almost unaffected (Figure 5a). After these 10 calcinations the

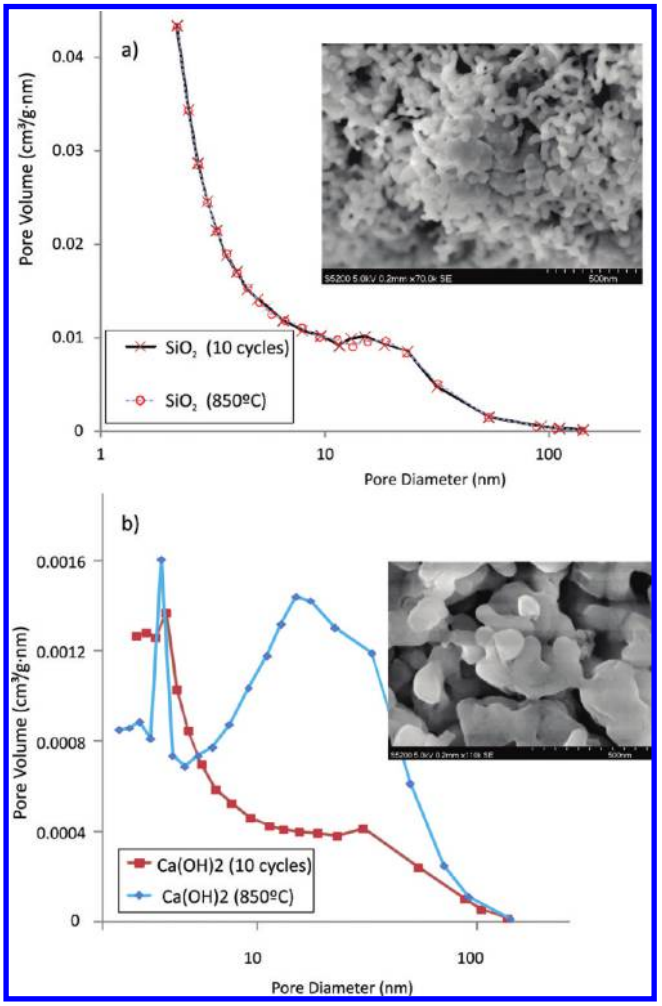

Figure 5. BJH desorption (dV/dD) pore volume distributions of nano-SiO_2 (a) and CaO (b) preheated at 850 °C and after 10 calcinations. The insets show SEM pictures of the samples after 10 calcination cycles.

BET surface area was 180 m^2/g, which is similar to the value obtained for the powder after first calcination. In contrast, the $Ca(OH)_2$ powder suffered a considerable decrease of the BET surface area: from 16.3 m^2/g for the powder as received down to 13 m^2/g after first calcination and 9 m^2/g after 10 calcinations (Figure 5b). The pore distributions of the mixtures were less distorted as the percentage of nano-SiO_2 was increased (inset of Figure 4b), which indicates that they have a higher thermal stability. From SEM images of the calcined mixtures (Figure 6a and 6b), regular cells (not visible in the calcined original sorbent) and reaction spots were observed. Figure 6c and 6d illustrate another feature observed in the modified samples after the TGA cycles, which is the development of surface cracks. An EDX spectrum of the surface of a calcined mixture is shown in Figure 6e. The X-ray mapping image shows Si and Ca local spots homogeneously distributed, indicating that SiO_2 and CaO have reacted during calcination. A well-defined peak in the EDX spectrum reveals

dx.doi.org/10.1021/es3002426 | Environ. Sci. Technol. 2012, 46, 6401−6408

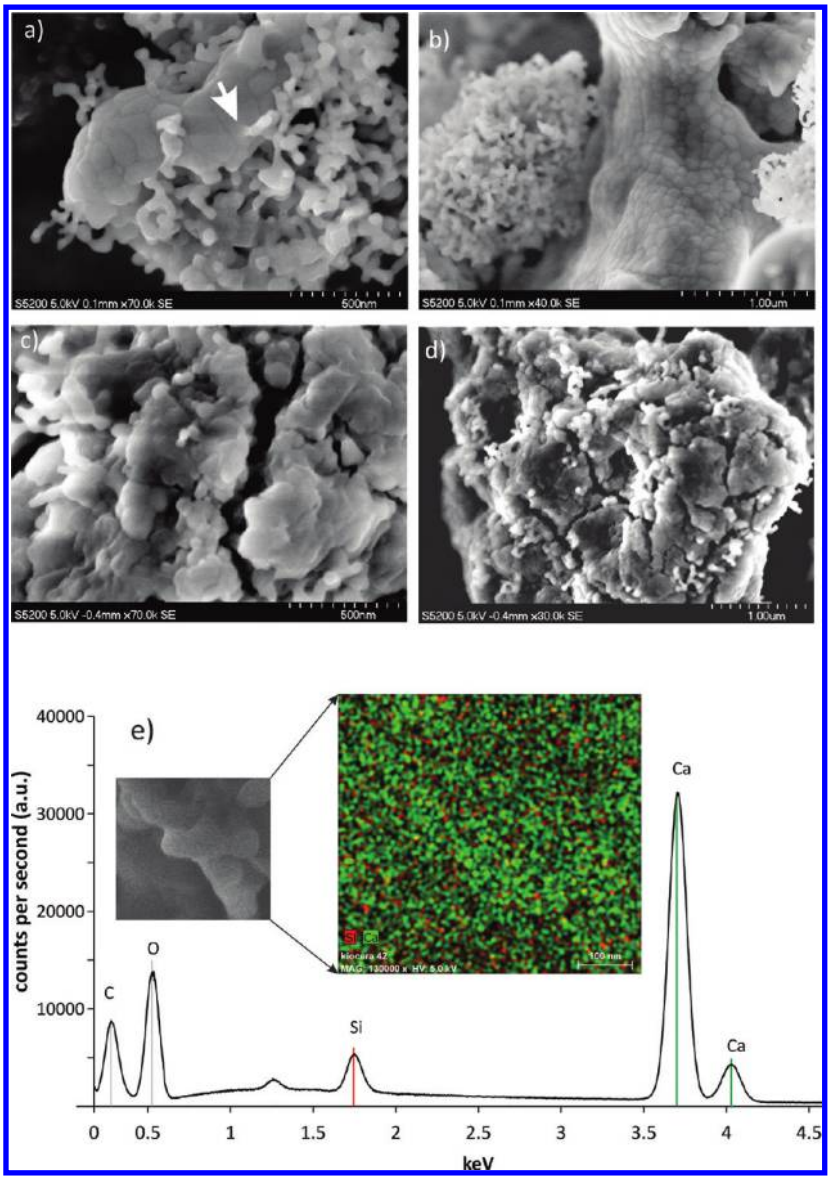

Figure 6. SEM pictures of a nano-SiO_2/CaO mixture: (a) after thermal pretreatment (the arrow indicates a reaction spot); (b) after 10 calcinations; (c) and (d) after 100 carbonation-calcination cycles. (e) EDX spectrum averaged on the region shown in the inset (500 × 500 nm^2) of a 10 times calcined mixture. The inset is an X-ray mapping image of the region shown, where green and red spots indicate the presence of Ca and Si, respectively. A quantitative mapping analysis yields a wt % of 9.7% for C, 2.5% for Si, 60.5% for Ca, and 27.3% for O.

also the presence of C, which suggests the occurrence of surface carbonation.

XRD analysis was performed on modified sorbent samples using a Bruker D8 Advance powder diffractometer equipped with a high temperature chamber, which allows for analyzing the samples under controlled atmosphere and temperature. Thermal pretreatment and a carbonation−calcination cycle was thus performed in situ. Temperature conditions were the same as in TGA tests. Preheating and calcination were performed in N_2 whereas carbonation was performed in CO_2. XRD patterns are shown in Figure 7 showing calcium silicate formation. During carbonation, most of the CaO was carbonated to $CaCO_3$, which subsequently decarbonated during calcination. On the other hand, the proportion of calcium silicates formed during preheating changed only slightly after carbonation and calcination as revealed by the quantitative Rietveld analyses performed on the XRD patterns (Figure 7c inset). Most of CO_2 sorption occurred thus by carbonation of CaO.

A general problem to apply the Ca-Looping process for postcombustion CO_2 capture is elutriation of fine particles at the typically high postcombustion gas velocities (above 1 m/s).[3] However, the effective particles in our preheated sorbent consist of large agglomerates wherein primary particles are strongly linked due to sintering at contacts. Particle size was measured by means of a Mastersizer 2000 (Malvern Instruments) based on laser diffraction of the sample dispersed in a fast-moving compressed air stream (10 kPa). A high-velocity air jet subjects the agglomerates to very high velocities (above 10 m/s), which might yield mechanical attrition.[22] The average particle size of the dispersed sample measured was 91 μm (volume weighted mean $D[4,3]$), which is similar to the particle size used in some Ca-looping pilot scale tests.[23] On the other hand, it must be remembered that the Ca-looping process also has an application in SE-SMR (sorption-enhanced steam methane reforming), where fluidized beds operate at lower gas velocities in the bubbling regime (~0.01−0.1 m/s).[5] With

dx.doi.org/10.1021/es3002426 | Environ. Sci. Technol. 2012, 46, 6401−6408

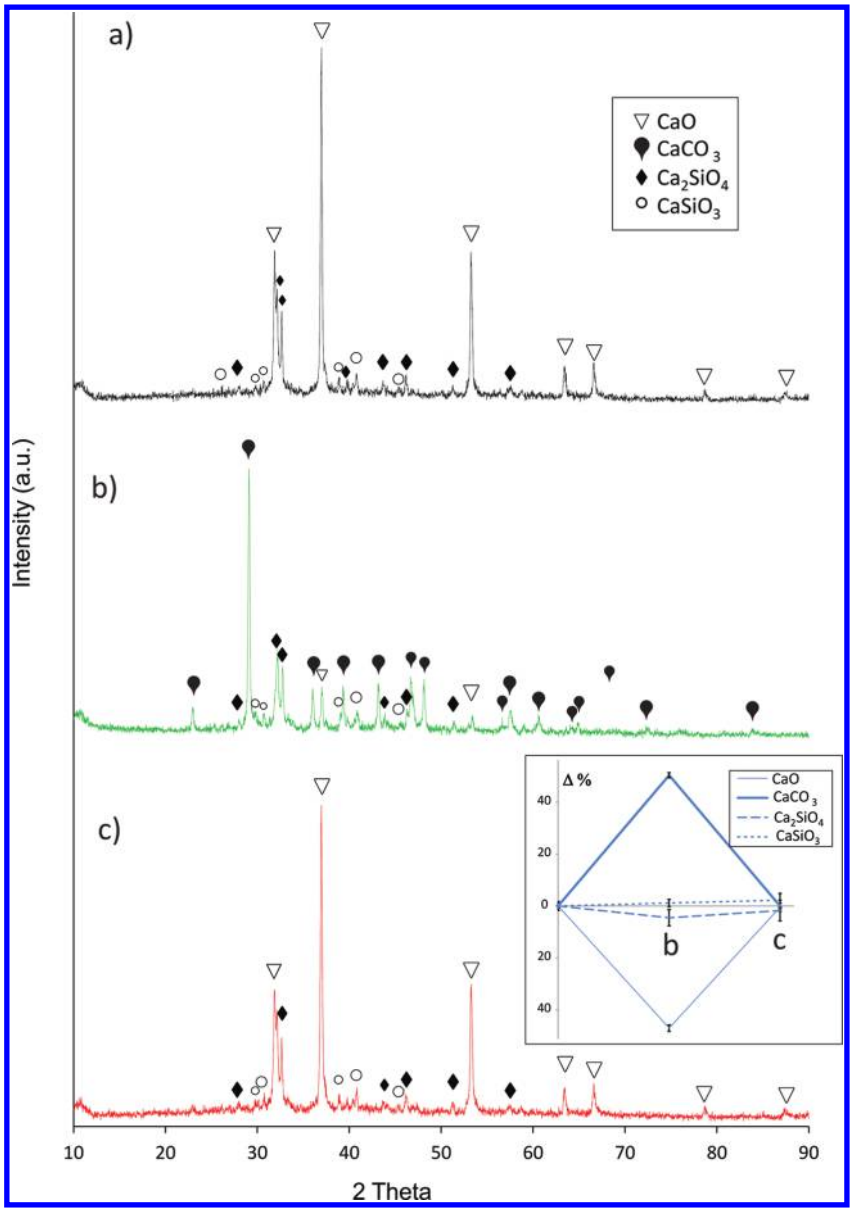

Figure 7. XRD patterns of a nano-SiO_2/CaO mixture preheated (a) and subjected to carbonation (b) and calcination (c) in situ in the DRX chamber at same temperature conditions and time periods as in TGA tests. The inset in (c) shows the variation of the composition percentages (measured by means of a Rietveld analysis) after carbonation (b) and calcination (c).

an average particle size close to 100 μm, elutriation of the preheated sorbent in a lab-scale bubbling bed was not significant as it was checked by performing a fluidization test. At a gas velocity of 0.12 m/s, the relative mass of powder elutriated from the bed ($\Delta m/m_0$) as a function of time t could be well fitted to the equation $\Delta m/m_0 = a(1-e^{-bt})$, where a = 0.0746, b = 0.1207, and t is in minutes (R_{sqr} = 0.998). After 1 min just about 1% of the initial mass (m_0 = 3.787 g) was elutriated.

3. DISCUSSION

Fast carbonation in sorbents with small pore size is limited by the lack of void space available for the growth of the carbonate layer in the kinetic regime.[24] Moreover, fast carbonation on the external surface of the large CaO agglomerates may give rise to a carbonate layer that blocks the transfer of CO_2 to the pores in the interior of these agglomerates. A main effect of nano-SiO_2 is to improve the dispersibility of CaO agglomerates. This would yield a larger number of reactive small pores directly exposed to CO_2, which otherwise would be placed in the interior of CaO agglomerates wherein the diffusive transfer of CO_2 is slow. The increase of the effective contact area to which CO_2 can be rapidly transferred would make fast carbonation proceed at a higher rate as seen in our results (Figure 2a). Even though the higher proportion of exposed small pores would enhance surface carbonation, these small pores become quickly saturated, which would explain the initially shorter duration of fast carbonation for the nano-SiO_2/CaO mixtures (Figure 2b). As the number of cycles is increased, the duration of fast carbonation is decreased at a larger rate for the CaO powder probably due to more intense sintering. The active small pores in the nano-SiO_2/CaO mixture would still allow for a relatively high contact area for fast carbonation as N increases due to thermal stability enhancement. This would contribute to lessen the progressive shortening of the fast carbonation period (Figure 2b) while the carbonation rate is kept still high as

dx.doi.org/10.1021/es3002426 | Environ. Sci. Technol. 2012, 46, 6401−6408

compared to the carbonation rate in CaO. In addition, surface structures and cracks observed in SEM images of the nano-SiO_2/CaO mixtures (Figure 6), which could be originated by the increase of molar volume associated with the formation of calcium silicates in the heated mixture, might contribute to further increase the effective surface area for carbonation.

Let us finally remark that the conditions used in the TGA runs were chosen to assess the sorbents performance as being close to conditions in the Ca-Looping process.[9] Manovic et al. have pointed out that it would be more realistic to test calcination at high CO_2 volume concentrations (80−90%) and higher temperature.[21,25] Under these harsher calcination conditions, the capture capacity of CaO is decreased due to enhanced sintering.[25] The results obtained here suggest that the effect of nano-SiO_2 will yield also a better performance when calcination is carried out at higher temperatures due to enhanced contact area and improved thermal stability. A detailed study of the performance of the mixtures as calcination conditions become harsher will be the subject of a separate work.

AUTHOR INFORMATION

Corresponding Author

*Phone: +34 954550960; fax: +34 954239434; e-mail: jmillan@us.es; mail: Department of Electronics and Electromagnetism, Faculty of Physics, Avda. Reina Mercedes s/n, 41012 Seville, Spain.

Notes

The authors declare no competing financial interest.

ACKNOWLEDGMENTS

This work was supported by the Andalusian Regional Government (Junta de Andalucia, contract FQM-5735) and Spanish Government Agency Ministerio de Ciencia e Innovacion (contracts FIS2011-25161 and CTQ2011-27626). We are grateful to Drs. MAS Quintanilla, M. J. Espin, and C. Soria-Hoyo for their help with sample preparation and characterization. We also acknowledge technical assistance from the Microscopy, X-ray, and Functional Characterization services of the Innovation, Technology and Research Center (CITIUS, University of Seville), and the Physisorption service of the Instituto de Ciencia de Materiales de Sevilla (CISC-Univ. Seville).

REFERENCES

(1) Abanades, J. C.; Anthony, E. J.; Lu, D. Y.; Salvador, C.; Alvarez, D. Capture of CO_2 from combustion gases in a fluidized bed of CaO. *AIChE J.* **2004**, *50* (7), 1614−1622.

(2) Alonso, M.; Rodriguez, N.; Gonzalez, B.; Grasa, G.; Murillo, R.; Abanades, J. C. Carbon dioxide capture from combustion flue gases with a calcium oxide chemical loop. Experimental results and process development. *Int. J. Greenhouse Gas Control* **2010**, *4* (2), 167−173.

(3) Blamey, J.; Anthony, E. J.; Wang, J.; Fennell, P. S. The calcium looping cycle for largescale CO_2 capture. *Prog. Energy Combust. Sci.* **2010**, *36* (2), 260−279.

(4) Wang, W.; Ramkumar, S.; Li, S.; Wong, D.; Iyer, M.; Sakadjian, B. B.; Statnick, R. M.; Fan, L. S. Subpilot demonstration of the carbonation-calcination reaction (CCR) process. High temperature CO_2 and sulfur capture from coal-fired power plants. *Ind. Eng. Chem. Res.* **2010**, *49* (11), 5094−5101.

(5) Johnsen, K.; Ryu, H. J.; Grace, J. R.; Lim, C. J. Sorption-enhanced steam reforming of methane in a fluidized bed reactor with dolomite as CO_2-acceptor. *Chem. Eng. Sci.* **2006**, *61* (4), 1195−1202.

(6) Bathia, S. K.; Perlmutter, D. D. Effect of the product layer on the kinetics of the CO_2-lime reaction. *AIChE J.* **1983**, *19* (1), 79−86.

(7) Grasa, G.; Murillo, R.; Alonso, M.; Abanades, J. C. Application of the random pore model to the carbonation cyclic reaction. *AIChE J.* **2009**, *55* (5), 1246−1255.

(8) Arias, B.; Abanades, J. C.; Grasa, G. S. An analysis of the effect of carbonation conditions on CaO deactivation curves. *Chem. Eng. J.* **2011**, *167* (1), 255−261.

(9) Grasa, G.; Gonzalez, B.; Alonso, M.; Abanades, J. C. Comparison of CaO-based synthetic CO_2 sorbents under realistic calcination conditions. *Energy Fuels* **2007**, *21* (6), 3560−3562.

(10) Chen, H.; Zhao, C.; Ren, Q. Feasibility of CO_2/SO_2 uptake enhancement of calcined limestone modified with rice husk ash during pressurized carbonation. *J. Environ. Manage.* **2012**, *93* (1), 235−244.

(11) Li, Y.; Zhao, C.; Ren, Q.; Duan, L.; Chen, H.; Chen, X. Effect of rice husk ash addition on CO_2 capture behavior of calcium-based sorbent during calcium looping cycle. *Fuel Process. Technol.* **2009**, *90* (6), 825−834.

(12) Wang, M.; Lee, C.-G.; Ryu, C.-K. CO_2 sorption and desorption efficiency of Ca_2SiO_4. *Int. J. Hydrogen Energy* **2008**, *33* (21), 6368−6372.

(13) Geldart, D. Types of gas fluidization. *Powder Technol.* **1973**, *7* (5), 285−292.

(14) Valverde, J. M.; Pontiga, F.; Soria-Hoyo, C.; Quintanilla, M. A. S.; Moreno, H.; Duran, F. J.; Espin, M. J. Improving the gas solids contact efficiency in a fluidized bed of CO_2 adsorbent fine particles. *Phys. Chem. Chem. Phys.* **2011**, *13*, 14906−14909.

(15) Hyeon-Lee, J.; Beaucage, G.; Pratsinis, S. E.; Vemury, S. Fractal analysis of flame synthesized nanostructured silica and titania powders using small-angle x-ray scattering. *Langmuir* **1998**, *14*, 5751−5756.

(16) Valverde, J.; Castellanos, A. Fluidization of nanoparticles: A simple equation for estimating the size of agglomerates. *Chem. Eng. J.* **2008**, *140* (1−3), 296−304.

(17) Quintanilla, M. A. S.; Valverde, J. M.; Espin, M. J. Electrofluidization of silica nanoparticle agglomerates. *Ind. Eng. Chem. Res.* **2012**, *51* (1), 531−538.

(18) Gallo, C. F.; Lama, W. L. Some charge exchange phenomena explained by a classical model of the work function. *J. Electrostat.* **1976**, *2* (2), 145−150.

(19) Grasa, G. S.; Abanades, J. C. CO_2 capture capacity of CaO in long series of carbonation/ calcination cycles. *Ind. Eng. Chem. Res.* **2006**, *45* (26), 8846−8851.

(20) Borgwardt, R. H. Sintering of nascent calcium oxide. *Chem. Eng. Sci.* **1989**, *44* (1), 53−60.

(21) Lu, D. Y.; Hughes, R. W.; Anthony, E. J.; Manovic, V. Sintering and reactivity of $CaCO_3$-based sorbents for in situ CO_2 capture in fluidized beds under realistic calcination conditions. *J. Environ. Eng.* **2009**, *135* (6), 404−410.

(22) Mueller, N.; Ecker, F. Determining granule breaking strength by laser diffraction method. *Pharm. Ind.* **2011**, *73* (11), 2061−2070.

(23) Gonzalez, B.; Alonso, M.; Abanades, J. C. Sorbent attrition in a carbonation/calcination pilot plant for capturing CO_2 from flue gases. *Fuel* **2010**, *89*, 2918−2924.

(24) Alvarez, D.; Abanades, J. C. Pore-size and shape effects on the recarbonation performance of calcium oxide submitted to repeated calcination/recarbonation cycles. *Energy Fuels* **2005**, *19*, 270−278.

(25) Manovic, V.; Charland, J.-P.; Blamey, J.; Fennell, P. S.; Lu, D. Y.; Anthony, E. J. Influence of calcination conditions on carrying capacity of CaO-based sorbent in CO_2 looping cycles. *Fuel* **2009**, *88*, 1893−1900.

View publication stats